AAPS PharmSciTech, Vol. 15, No. 4, August 2014 (© 2014)
DOI: 10.1208/s12249-014-0129-4

Research Article

Nanoemulsion for Solubilization, Stabilization, and *In Vitro* Release of Pterostilbene for Oral Delivery

Yue Zhang,[1,2,3] Zhenhua Shang,[1,2,3,5] Chunhui Gao,[4] Man Du,[1] Shixia Xu,[1] Haiwen Song,[1] and Tingting Liu[1]

Received 17 December 2013; accepted 10 April 2014; published online 15 May 2014

Abstract. Pterostilbene, being extracted from many plants, has significant biological activities in preventing cancer, diabetes, and cardiovascular diseases so as to have great potential applications in pharmaceutical fields. But the poor solubility and stability of pterostilbene strictly restrained its applications. As a good protection and oral delivery system, an optimal nanoemulsion for pterostilbene was developed by using low-energy emulsification method. Systematic pseudo-ternary phase diagrams have been studied in optimization of nanoemulsion formulations. The prepared pterostilbene nanoemulsion was characterized by transmission electron microscope, Fourier transform Raman spectrum, and laser droplet size analyzer. Nanoemulsion droplets are circular with smooth margin, and the mean size is 55.8± 10.5 nm. The results illustrated that the nanoemulsion as oral delivery system dramatically improved the stability and solubility of pterostilbene, and *in vitro* release of pterostilbene was significantly improved (96.5% in pH 3.6 buffer; 13.2% in pH 7.4 buffer) in comparison to the pterostilbene suspension (lower than 21.4% in pH 3.6 buffer; 2.6% in pH 7.4 buffer).

KEY WORDS: 3,5-dimethoxyl-4′-hydroxystilbene; nanoemulsion; pseudo-ternary phase diagram; pterostilbene; release study.

INTRODUCTION

Pterostilbene (*trans*-3,5-dimethoxyl-4′-hydroxylstilbene, structure shown in Fig. 1), a kind of phytoalexin and belonging to the stilbenoid compound (1), was found existing in many plants and fruits. When first isolated from red sandalwood (2), pterostilbene was extracted from *Pterocarpus santalinus* (3) and in succession found in proplis (4), leaves of *Vitis vinifera* (5), dark red heart wood of *Pterocarpus marsupium* (6), Vaccinium berries (7), fungal-infected grape berries of varieties Chardonnay, Pinot Noir (8), *Dracaena cochinchinensis* (Lour.) in China, Yunnan (9) and Jacareubin in Brazil (10). Pterostilbene has over the years attracted the attentions of researchers due to the broad range of biological activities. In India, pterostilbene was used in Ayurvedic medicines which are known as age-old herbal preparations, being prescribed for diabetes, cardiotonic, and other disorders (11). Recent researches revealed that pterostilbene had great effect on inducing HeLa cell apoptosis in human neutrophils (12), preventing azoxymethane (AOM)-induced colon tumorigenesis (13,14) and anti-cancer abilities including gastric cancer cells (15), B16 melanoma cells (16), multi-drug resistant leukemia cells (17), lung cancer cells (18), and breast cancer cells (19). Obviously, pterostilbene has great potential value in the applications of pharmaceutical and nutrition food, but the poor water solubility and stability of pterostilbene would seriously limit its applications and *in vivo* bioavailabilities. Especially, pterostilbene is unstable with light and air because phenolic hydroxyl can be easily oxidized and its *trans* configuration can transform to *cis* configuration which exhibits no significant activity. Hence, it is important to find a suitable delivery system for improving the solubility and stability of pterostilbene to gain the reasonable biological effect.

Nanoemulsions are non-equilibrium system and possess kinetic stability in a long period with a remarkable small droplet size (below 200 nm) (20). It is a most concerned delivery system in pharmaceutical applications because of the ability of solubilizing water-insoluble drugs (21) and the intensified bioavailability of drugs by dispersing them into extremely small particles to greatly increase the solubility and permeability of drugs (23,24). Drug placed in nanoemulsion droplet is free from air, light, and hard environment; therefore, as a delivery system, nanoemulsion can not only improve the bioavailability of drugs but also protect them from oxidation and hydrolysis, while it possesses an ability of sustained release at the same time (22). Nanoemulsions can be prepared by methods of high-energy emulsifying and low-energy emulsification which include phase inversion composition (PIC), phase inversion temperature (PIT), and self-emulsifying method (25). The low-energy emulsifying method possesses great advantages of lesser physical destruction of

[1] School of Chemical and Pharmaceutical Engineering, Hebei University of Science and Technology, Shijiazhuang, 050018, China.
[2] Hebei Research Center of Pharmaceutical and Chemical Engineering, Shijiazhuang, 050018, China.
[3] State Key Laboratory Breeding Base-Hebei Province Key Laboratory of Molecular Chemistry for Drugs, Shijiazhuang, 050018, China.
[4] Zizhu Pharmaceutical, Qinhuangdao, 066004, China.
[5] To whom correspondence should be addressed. (e-mail: zhenhuashang@126.com; zhenhuashang@126.com)

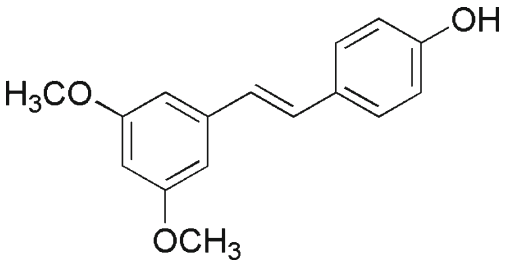

Fig. 1. Structure of pterostilbene

active agents, smaller size of droplets, better phase behavior, and more convenient industrial scale-up than high-energy emulsifying methods (26–28). Of the low-energy emulsifying methods, PIC method has been the most commonly used. In the PIC process, the stability and droplet size are greatly influenced by oil/surfactant ratio, hydrophile-lipophile balance (HLB) of surfactants, and fractions of components in the system (29,30). In general, optimum formulation was selected on the basis of pseudo-ternary phase diagrams. The nanoemulsion region would be the basis for the selection of the formulation (31).

The present study aimed at developing an optimal O/W pterostilbene nanoemulsion by the PIC method on the basis of minimum surfactant concentration with increases the solubility, stability, and the release performance of pterostilbene. The nanoemulsion as a drug delivery system for pterostilbene, including the formulation and *in vitro* release evaluation, has not been reported by literature so far.

MATERIALS AND METHODS

Pterostilbene (99%, HPLC) used in this study was synthesized in our laboratory according to the literature (32). Polyoxyethylene sorbitan fatty acid esters (Tween-80) and polyoxyethylenated castor oil (EL-40) were purchased from Tianjin Guangfu Chemical Reagent Development Center, Tianjin, China. Fatty alcohol-polyoxyethylene ether (AEO-7) was bought from Jinpeng Chemical Co., Shijiazhuang, China. Isopropyl myristate (IPM) was bought from Shanghai Leasun Chemical Co. Ltd., Shanghai, China. Methanol used in HPLC was chromatographically pure and purchased from Kangkede Co., Tianjin, China. Other chemical reagents were all of analytical grade and purchased from Modern Reagent Co., Shijiazhuang, China. Oils were all of food grade and purchased from COFCO, Tianjin, China. Dialysis bags were bought from Yuanye Biological Science Company, Shanghai, China. Chemical reagents and oils were used directly without further purification. Water was twice distilled.

Solubility Tests

The excess amount of pterostilbene was added to 2 mL of each selected component (or a nanoemulsion system) in a stoppered vial at 37±1°C for 72 h, respectively. Then, the vials were centrifuged at 3,000 rpm for 15 min. To determine the maximum solubilities of pterostilbene in different components, triplicated supernatants were measured by HPLC.

Selection of Surfactant and Cosurfactant

Pseudo-ternary phase diagrams were constructed by aqueous titration method. Certain amount of pterostilbene dissolved in cosurfactant in a vial at 25±5°C. The solution of cosurfactant and pterostilbene was dropped into the vial containing oil medium and surfactant and was thoroughly mixed. Water was added continuously to the above mixture. As water amount increases, the system varied from clear to viscous, and liquid crystals appeared. In proceeding with the addition of distilled water, the system changed from viscous to a stable, colorless, and transparent or translucent liquid with Tyndall effect being observed. These bluish and transparent mixtures were designated as nanoemulsions, and opaque mixtures were designated as normal emulsions (33). Note down the mass percentage of all components corresponding to the phase inversion point where the system changed from clarity to turbidity or from clarity to thickness or back again from thickness to clarity. Physical states of emulsions were marked on a pseudo three-component phase diagrams, with one axis representing the aqueous phase, the other one representing oil, and the last one representing a mixture of surfactant and cosurfactant at fixed mass ratios.

IPM was used as the oil phase on the basis of former solubility studies. In view of the soluble ability of three surfactants at the same order of magnitude gained from the former studies, they were all used as surfactant candidates in a formulation screening test. The surfactant candidates matched with different cosurfactants to look for a better combination. The common cosurfactants used in the oral formulation are alcohols with a short carbon chain. We chose ethanol, ethylene glycol, i-propanol, 1,2-propylene glycol, and *n*-butanol as cosurfactants. Three surfactants were composite grouped with cosurfactant candidates basing on specific mass ratios of surfactant and cosurfactant (Km) from 1:9, 2:8, 3:7, 4:6, 5:5, 6:4, 7:3, 8:2 to 9:1, respectively, with the total quantity of mixture being 1.0 g. The mass ratio of IPM to the mixture of surfactant with cosurfactant (Smix) at specific Km was also varied from 1:9, 2:8, 3:7, 4:6, 5:5, 6:4, 7:3, 8:2 to 9:1 for phase studies. Surfactant and cosurfactant were screened depending on the nanoemulsion region and range of mass ratio from each of the constructed phase diagram. First, the mass ratio of Smix to oil (IPM) was fastened to 9:1 to observe the formation of nanoemulsion with the value of Km changing. The surfactant possessing a strong emulsifying ability with several cosurfactants under a wide range of Km was selected to be used in the formulation. Second, the phase diagrams were established by changing the mass ratio of Smix to IPM under several fixed Kms, and the screening of cosurfactant was depended on the size of the nanoemulsion region.

After the screening of surfactant, cosurfactant and a preliminary selection of Km on the basis of phase diagrams were conducted. Surfactant (EL-40) was coupled with ethanol in four groups under different fixed mass ratios of Km (6:1, 5:1, 4:1, or 3:1), and the total quantity of mixture was still maintained to 1.0 g. For each group, IPM was added and mixed well with surfactant and cosurfactant. The mass ratio of Smix to oil was kept ranging from 1:9, 2:8, 3:7, 4:6, 5:5, 6:4, 7:3, 8:2 to 9:1. Phase diagrams under different fixed mass ratios of Km (6:1, 5:1, 4:1, or 3:1) were developed.

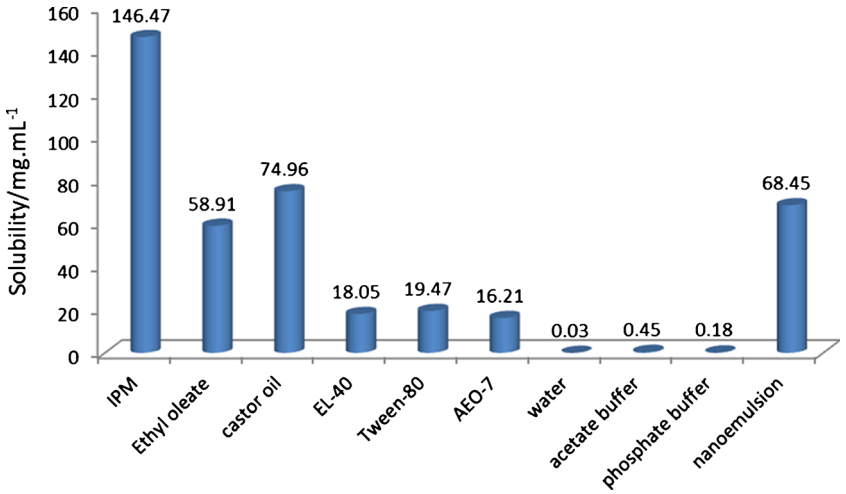

Fig. 2. Solubilities of pterostilbene in different components and nanoemulsions, $n=3$

Screening for an optimal nanoemulsion formulation, particle size distribution is another important problem because the small size of droplet is in favor of the dispersity and bioavailability of the drug. Km and mass ratio of Smix to oil were needed to adjust so as to obtain an optimal formulation possessing an ideal particle size in a narrow distribution. Basing on the former selection, Km and the ratios of Smix to oil were changed in a narrow range to observe the size distributions of a droplet.

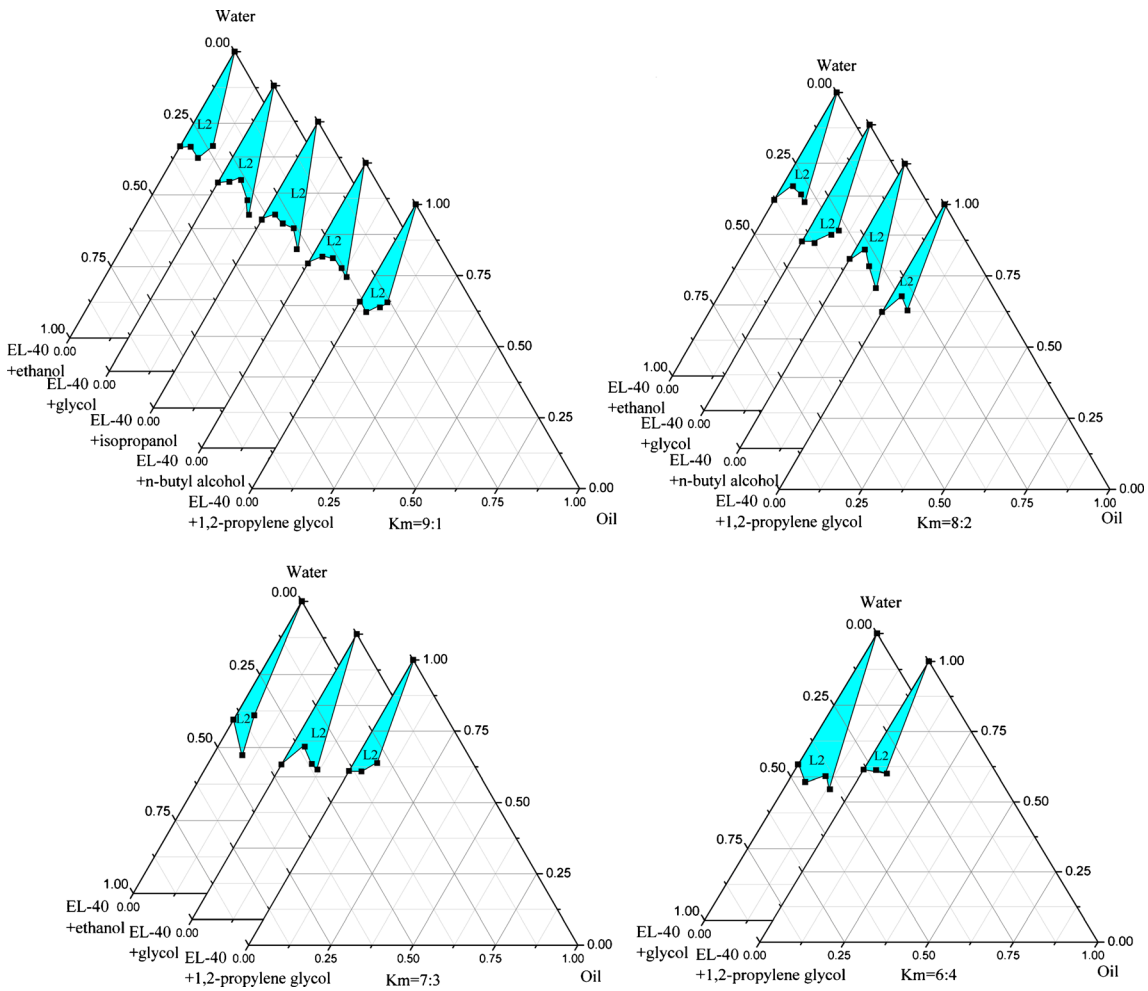

Fig. 3. Ternary phase diagrams of selected nanoemulsion at fixed Km; *L2* O/W nanoemulsion area

Determination of Physico-chemical Parameters

The type of nanoemulsion was identified by a staining method with observing diffuse velocity of staining agents methylthionine chloride and Sudan red (34). Transmission electron microscopy (TEM, H-7650, Hitachi, Japan) was used to monitor the morphology of nanoemulsion droplets. The nanoemulsion was diluted for 400 times by water and dyed by phosphomolybdic acid. The sample was observed on the copper grid. Droplet size distribution was determined by a laser scattering analyzer (Nano-S90; Malvern, UK). Samples were diluted for 400 times by water and observed at absorbance and refractive index beings. Fifty microliters of the prepared nanoemulsion were diluted with water to 20 mL. The light-scattering angle was recorded at 90°, and temperature was maintained at 25°C. During the measurement, average particle count rate was maintained between 50 and 500 kcps. Fourier transform Raman analyses were performed on a FT-Raman spectroscopy (MultiRam, Bruker, America) at a laser 350-mW scanning from 50 to 4,000 cm^{-1}. The amount of pterostilbene in experiments of solubility, stability, and *in vitro* release was detected by HPLC (LC-20AT VP, Shimadzu, Japan). The mobile phase was a mixture of methanol and distilled water (V/V=60/40). The HPLC column was a Phenomenex Luna-C18 (250×4.6 mm, 5 μm). The flow rate was 1.0 mL•min^{-1}, the detection wavelength was 319 nm, and the sample injection volume was 10 μL. The value of pH was determined by acidimeter (pH-FE20, Mettler Toledo, Switzerland). Refractive index was measured by Abbe refractometer (WYA-2s, Kaertesi, China). Viscosity of nanoemulsion was directly examined without dilution by a viscosimeter (DV-II, Brookfield, America).

Stability Assessment

In order to observe the stability of the prepared formulation and avoid metastable system, various stability studies like bearing centrifugation, heat, humidity, and light irradiation were investigated. After centrifugation, if no instability of pterostilbene nanoemulsion such as phase separation, cracking, or creaming was observed, it would be assessed with other stabilities according to the regulations of Chinese Pharmacopoeia (35) including high-temperature, high-humidity, and hard light irradiating tests. The prepared pterostilbene nanoemulsion was performed, centrifuging test at 10,000 rpm for 2 h and followed by an examination for phase. Then, nanoemulsion was kept at a certain circumstance of 60±2°C, RH 92.5±5%, or hard light irradiating (4,500±500 lx) for specific times. Samples were withdrawn after specified time intervals (0, 5, and 10 days) and examined for phase separation, mass variations under high humidity, and contents of pterostilbene under high temperature and hard light irradiating. In addition, the droplet size of nanoemulsion was observed under the same conditions.

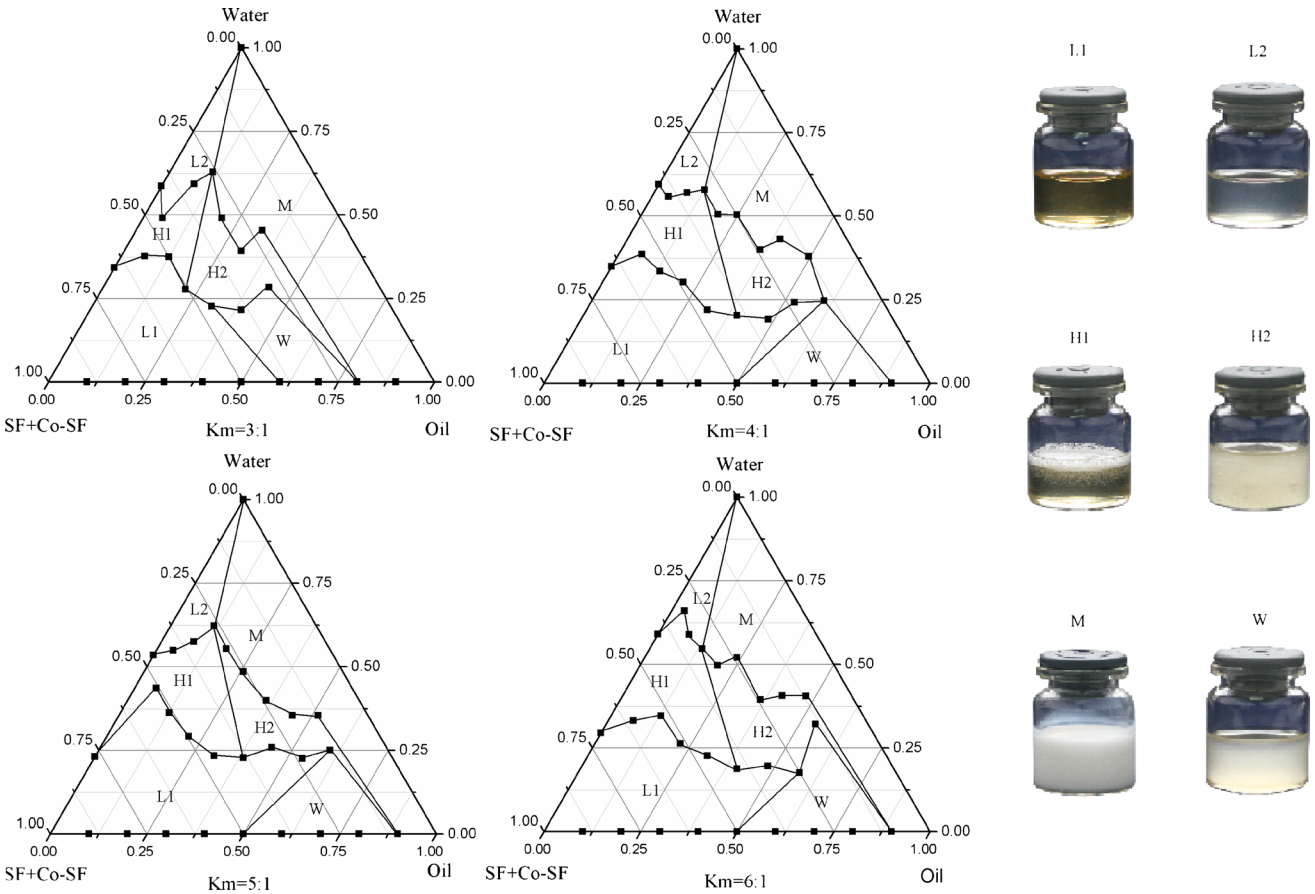

Fig. 4. Pseudo-ternary phase diagrams indicating O/W nanoemulsion region at different Km ratios; *L1* W/O nanoemulsion area, *L2* O/W nanoemulsion area, *H1* viscous but clarified area, *H2* viscous but opacified area, *M* ordinary emulsion area, *W* turbid area

Table I. Physico-chemical Parameters of Nanoemulsion (Mean±S.D., $n=3$)

Parameter	Results
Structure type	O/W
pH	5.87±0.01
Refractive index	1.3841±0.002
Viscosity/mPa·s	241.3±0.02
Mean size/nm	55.8±10.5

O/W oil/water nanoemulsion

In Vitro Release Performances

Two milliliters of nanoemulsion (containing about 30 mg of pterostilbene) was mixed with 1-mL acetate buffer solution (ABS) or phosphate buffer solution (PBS) simulating gastric and intestinal conditions in a dialysis bag (Spectrum MW1000). The bag was placed in a shaking basket which was immersed in 60-mL ABS or PBS at 37±0.5°C with continuous shaking. In accordance with the selected time intervals (0.5, 2, 6, 10, 12, 18h, 24, 36 h), 5 mL of release medium was taken out, and the equivalent fresh buffer solution which had been warmed at 37±0.5°C was added to maintain the total volume unchanged. The content of pterostilbene in samples was analyzed by HPLC, and the accumulating release degree was calculated. Release behavior of nanoemulsion was compared with that of plain pterostilbene suspension (30 mg of pterostilbene).

RESULTS

The soluble performances of pterostilbene in different components and nanoemulsion are shown in Fig. 2.

Figures 3 and 4 are a visualized disclosure of the emulsification efficiency of Smix with oil in several settled Kms.

The physico-chemical properties and morphology of nanoemulsion are shown in Table I and Fig. 5, respectively. Nanoemulsion droplets are circular with smooth margin. Light color on the edge of the droplet is a shell caused by the orient arrangement of surfactants, and the darken core means that pterostilbene is embedded.

FT-Ramon spectroscopy is used to determine the nanoemulsion due to the faint Raman scattering of water and having non-destructive impact on nanoemulsion. As shown in Fig. 6, because the surfactant (EL-40) and cosurfactant (ethanol) have no clear characteristic scattering absorbance, pterostilbene and nanoemulsion have almost the same scattering peaks. The scattering characteristic peak of weak aromatic C–H vibrating appears at 3,035 cm^{-1}. The intensified peaks of nanoemulsion from 2,800 to 3,100 cm^{-1} are observed owing to many methyl and methylene groups existing in surfactant and cosurfactant. The scattering characteristic peaks at 1,587 and 1,631 cm^{-1} are attributed to the conjugating aromatic ring of stilbene and trans-double carbon bond, respectively. There is an out-of-plane bending vibration peak of *trans*-arylolefin at 995 cm^{-1}, and the peak of 1,280 cm^{-1} indicates that methoxyl groups of pterostilbene exist. FT-Raman spectra illustrated that the drug encapsulated in nanoemulsion droplets is pterostilbene.

After centrifugation at 10,000 rpm for 2 h, any creaming, cracking, crystal precipitation, or phase separation was not found, indicating an excellent phase stability of the nanoemulsion. The results of other hard condition stability tests are shown in Table II.

The dynamic dialysis method was applied in the *in vitro* release test of nanoemulsion. Data obtained here were managed by calibration curve method to acquire a concentration corresponding to each time interval. The accumulated amount of pterostilbene released from the dialysis bag was obtained from Eq. 1.

$$\mathrm{Qt} = C_1 V_0 + (C_{0.5} + C_1 + \ldots + C_{t-1})\ V \tag{1}$$

Where Qt stands for the accumulated amount of pterostilbene released from the dialysis bag; Ct is defined as the concentration of pterostilbene at t (time) in nanoemulsion

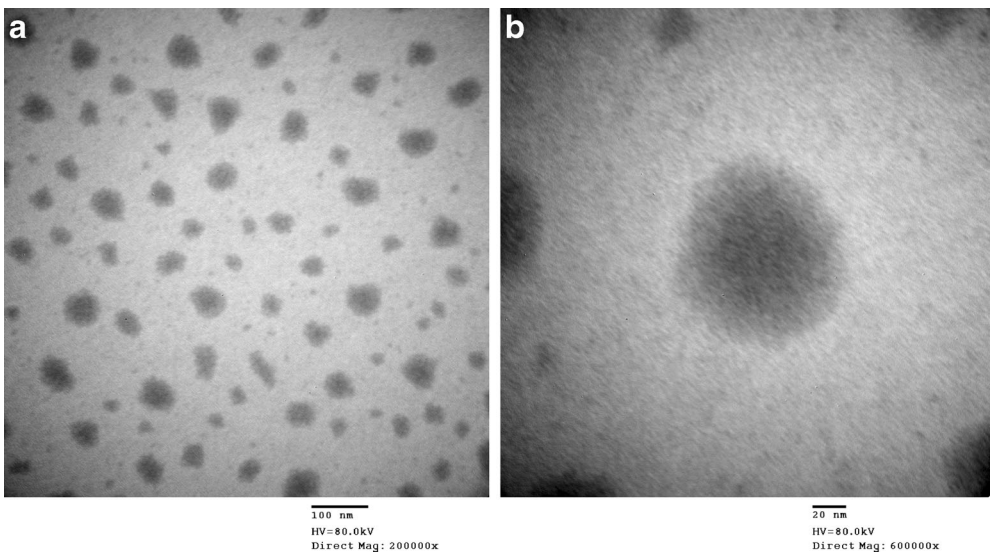

Fig. 5. TEM of pterostilbene nanoemulsion

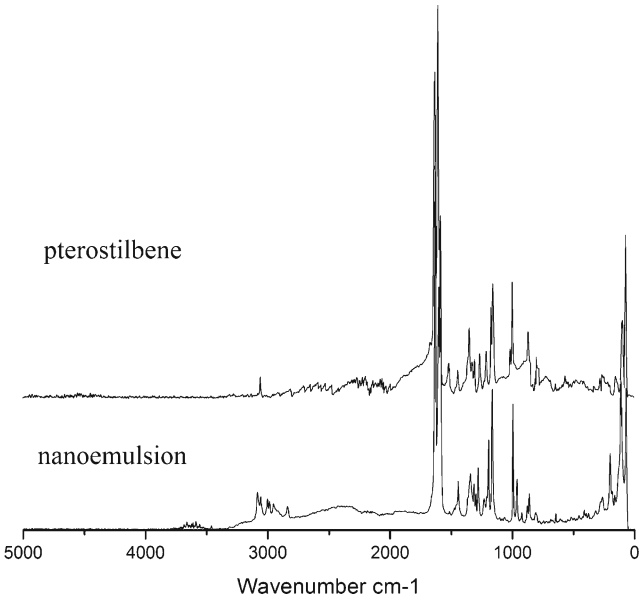

Fig. 6. FT-Ramon spectra of pterostilbene and nanoemulsion

or pterostilbene suspension in buffers; V_0 is the total volume of buffer solution; V is the volume of sample being taken out. The performances of *in vitro* release under different conditions are shown in Fig. 7.

DISCUSSIONS

Solubility of drug has a great influence on nanoemulsion formulation (33). Therefore, it is necessary to realize the solubilities of pterostilbene in different agents, including oil media, non-ionic surfactants, and water. Oils frequently used such as castor oil, IPM, and ethyl oleate were selected as oil candidates in the formulation. HLB of surfactant closely related with the selection of the suitable emulsifier for a given oil phase and should be seriously considered (36). If the HLB of emulsifier could match well with oil, the best emulsification would be realized, and nanoemulsion would be formed with much small droplets (37). For obtaining oil/water (O/W)-type nanoemulsion, the HLB of emulsifier should be from 8 to 18. Therefore, non-ionic surfactant candidates EL-40, Tween-80, and AEO-7 with HLB values of 13, 15, and 12, respectively, were selected as surfactants in this experiment, and determination of oil phase would depend on the solubilities of pterostilbene because a high solubility of drug in the oil phase implies a strong carrying capacity of drug in the solubilized form of the nanoemulsion. As seen from Fig. 2, IPM shows considerable soluble ability for pterostilbene and was selected as the oil phase. Here, three kinds of surfactants (EL-40, Tween-80, and AEO-7) also show an acceptable solubility of pterostilbene; and on further studies, the favorite one will be selected. As illustrated by the results, pterostilbene showed extremely poor solubilities in water, acetate buffer, and phosphate buffer, this enhances the importance of developing a new delivery system for pterostilbene. The nanoemulsion formulation consisted of surfactant, oil, and drug should have a good solubility for the drug (27). Also shown in Fig. 2, the solubility of pterostilbene in the selected model nanoemulsion formulation is approximately 2,200 times of that in water. Therefore, the solubility of pterostilbene was greatly enhanced by nanoemulsion.

A binding of surfactant and cosurfactant possessing an appropriate HLB value contributes to adjusting the interfacial tension to acquire a favorable emulsifier (38,39). HLBs of AEO-7, EL-40, and Tween-80 range from 12 to 16, considering the biocompatibility; all these three components can be used as surfactant candidates in O/W nanoemulsion formulations. Pseudo-ternary phase diagram is an intuitionistic method to realize a preliminary screening of surfactant and cosurfactant for nanoemulsion formulation. A range of cosurfactants can be arranged in pairs with surfactants, and the emulsification efficiency (nanoemulsion region area) would come to the selection perspective. As seen from Fig. 3, when IPM is selected as oil phase, EL-40 and Tween-80 can arrange more kinds of cosurfactants in pairs to generate nanoemulsion than AEO-7, and EL-40 matches well with ethanol, ethylene glycol, or 1,2-propylene glycol in a wider range of Km than AEO-7 or Tween-80. Although EL-40 has the best performance of all the cosurfactants, ethylene glycol was still discarded due to the risk of its potential biological toxicity. *n*-Butyl alcohol has a larger nanoemulsion region at Km of 9:1 or 8:2, but no phase inversion appears at Km of 7:3 or 6:4. Although 1,2-propylene glycol enjoys considerable advantage over ethanol in Km (6:4), it cannot compete with ethanol in the stability of formed nanoemulsion. In a subsequent study, nanoemulsion prepared by using 1,2-propylene glycol was not good enough to store because of pterostilbene flocculation and precipitation from nanoemulsion after 20 days. Ethanol is the most readily available cosurfactant with no irritation and toxicity to human body and has justifiable performance with

Table II. Stabilities of Pterostilbene Nanoemulsion (Mean±S.D., $n=3$)

	Mass/g	Content/%				
Test items	Pterostilbene	Nanoemulsion	Pterostilbene	Suspension[a]	Nanoemulsion	Mean size/nm
0 day	10.4819±0.0011	11.3476±0.0021	99.2±0.1	99.2±0.1	99.2±0.1	57.13±5.67
60°C, 5 days	–	–	97.9±0.2	97.3±0.1	98.7±0.1	58.07±4.65
60°C, 10 days	–	–	97.4±0.1	97.0±0.1	98.5±0.2	59.55±7.83
92.5% humidity, 5 days	10.4825±0.0017	11.3480±0.0019	–	–	–	57.94±5.82
92.5% humidity, 10 days	10.4838±0.0020	11.3482±0.0015	–	–	–	58.94±6.78
4,500±500 lx, 5 days	–	–	96.2±0.2	96.0±0.1	98.0±0.3	58.01±3.95
4,500±500 lx, 10 days	–	–	95.8±0.2	94.6±0.1	97.9±0.1	58.89±5.94

[a] Pterostilbene was suspended in water

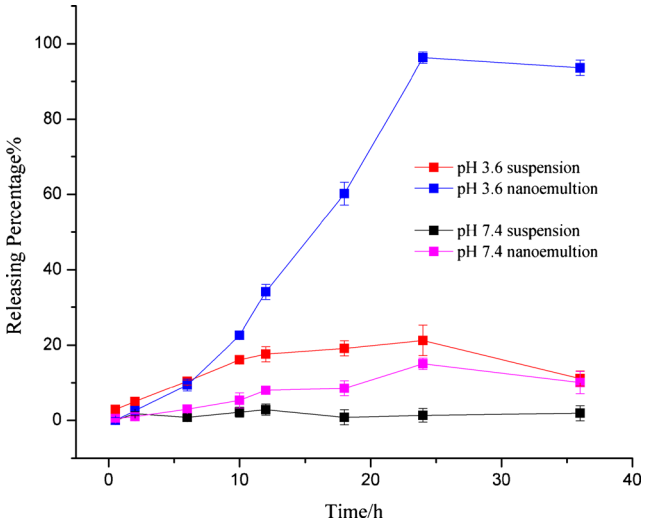

Fig. 7. *In vitro* release tests of pterostilbene and nanoemulsion in different buffer solutions, $n=3$

being arranged EL-40 in pairs to generate phase inversion. With taking a comprehensive view, we select EL-40 as the surfactant and ethanol as the favorable cosurfactant to develop the nanoemulsion formulation.

As seen from Fig. 4, when Km was adjusted to 3:1, the maximum amount of emulsified oil is 11.1% (*w*/*w*) with Smix of 25.9% (*w*/*w*); the nanoemulsion region somewhat extends with Km increasing to 4:1, and the amount of oil emulsified increases slightly near to 12.6% (*w*/*w*) with Smix of 29.4% (*w*/*w*); however, when Km is adjusted to 5:1, the maximum amount of oil that can be emulsified decreases to 11.3% (*w*/*w*) with 26.4% (*w*/*w*) of Smix. Upon further increasing the proportion of surfactant to Km of 6:1, it is observed that the amount of oil emulsified slightly increases again to 13.5% (*w*/*w*) with Smix of 31.7% (*w*/*w*). Although a largest amount of oil can be emulsified when Km is taken as 6:1, in comparison with the other three, the region of nanoemulsion is the smallest. The largest nanoemulsion area appears when Km is taken as 3:1, but the amount of oil that can be emulsified is not enough (11.1%). The other two almost have the equal area but possess very different ability of emulsion. According to the nanoemulsion region areas reflected by phase diagrams and the amount of oil emulsified by minimum amount of emulsifier, we preliminarily selected the Km as 4:1.

The mass ratio of Smix to oil under a sort of fixed Km is a main factor impacting on the size of droplet. Increase of emulsifier would result in increased adsorption around the oil-water droplet interface and decreased interfacial tension in the system to form nanoemulsion with smaller droplets (40). For the ideal droplet size distribution, the interfacial tension, which is directly relevant to Km and ratio of Smix to oil, should be adjusted to a favorable level. With the preliminary selected Km (4:1), nanoemulsion were prepared separately at different mass ratios of Smix to oil (3:1, 4:1, 5:1), and size distributions of droplets observed by light-scattering studies are shown in Fig. 8. At the mass ratio of Smix to oil of 3:1, the particle size distribution is showed as two branches, one branch with considerable amount of droplets in the range of 25–70 nm, the other branch with a range of 4,000–7,000 nm, implying that oil cannot be completely emulsified due to the deficiency of emulsifier. At a mass ratio of Smix to oil of 4:1, the nanoemulsion possesses a narrow droplet size distribution, and the mean size is 55.8 nm. Trying to get smaller droplets, the mass ratio of Smix to oil is adjusted to 5:1; there are two branches that appeared, and the mean droplet size decreases to 27.6 nm, with one of the branches in the range below 10.0 nm, it is still unreasonable because the droplet is too small to encapsulate pterostilbene. Upon further increasing the mass ratio to 6:1, two branches are still obtained, indicating a sharp decrease in interfacial tension. Overdose of emulsifier would produce a liquid crystalline phase leading to a higher droplet size when IPM was used as oil, it has been reported elsewhere (41). Therefore, under the fixed Km (4:1), the favorable mass ratio of Smix to oil is selected as 4:1.

An O/W nanoemulsion formulation containing EL-40 33.6%, ethanol 8.4%, IPM 10.5%, and water 47.5% (mass ratio) was selected based on pseudo-ternary phase diagram, stability, optimum droplet size, and lower concentration of emulsifier, contributing to lower toxicity for oral administration.

As seen from Table II, mass loss of nanoemulsion under high humidity condition after 10 days is rather small compared with that of plain pterostilbene. The content of plain pterostilbene after 10 days varied clearly under high temperature and hard light irritation test, so the number is 1.8 and 3.4%. Especially, the content tended to decrease rapidly when pterostilbene was suspended in water after 10 days. On the contrary, nanoemulsion is more stable, and the decreases of content are 0.7 and 1.3%, respectively, at the same conditions. In addition, there is no phase separation, and the size distribution of droplets has no clear variation under all the test items. Therefore, nanoemulsion as a delivery system for pterostilbene has a great advantage on improving the stability of pterostilbene.

Pterostilbene suspension shows an unsatisfied releasing results neither in ABS (pH 3.6) nor in PBS (pH 7.4), with

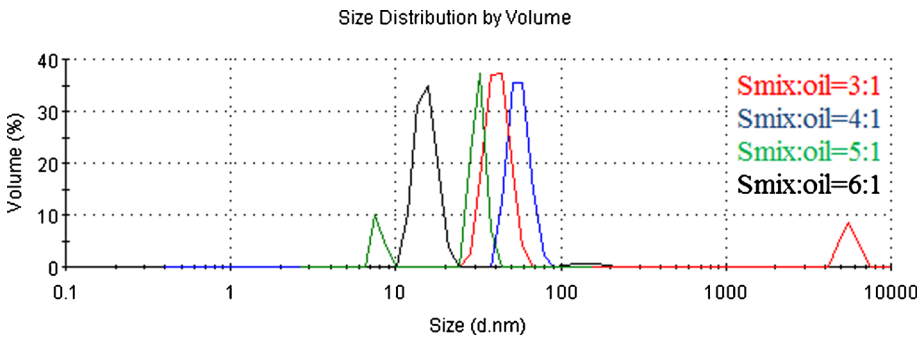

Fig. 8. Size distribution studies of nanoemulsion under different ratios of Smix to oil (Km=4:1)

21.23 and 2.81%, respectively, within 24 h. It may be caused by the poor solubility of pterostilbene in water and buffers (seen from Fig. 2). In comparison, the maximum release of pterostilbene from nanoemulsion in ABS (pH 3.6) can achieve 96.25% in 24 h; more than 60% of pterostilbene is released from nanoemulsion in the initial 20 h. After 30 h, the release of pterostilbene from nanoemulsion reduces, it is probably caused by the degradation of pterostilbene because many impurity peaks were detected by HPLC. In PBS (pH 7.4), the release of nanoemulsion is also significantly improved, the maximum release increases from 2.81 to 15.05% within 24 h. In comparison, though degrading happened at the same time (24 h) in ABS (pH 3.6), the decreased ratio of nanoemulsion (about 2.8%) is markedly lower than plain pterostilbene suspension (about 47.57%) within 36 h; in PBS (pH 7.4), the degradation of pterostilbene suspension happened at 12 h whereas of nanoemulsion is observed at 24 h. The unsatisfactory result at pH 7.4 is likely caused by the lower soluble performance at pH 7.4 than at pH 3.6. Low solubility may lead to congestion of the membrane channel resulting in a small amount of release. Equilibrium of dialysis may be another reason for a less release because it would limit the release from the bag. Even so, comparing with the control pterostilbene, it is obvious that nanoemulsion, as a delivery system, significantly improves the release performance of pterostilbene, and it is further expected to effect on the bioavailability of pterostilbene.

CONCLUSION

Nanoemulsion, used as a delivery system to improve the solubility, stability, and control release of pterostilbene, was investigated in this paper. Pterostilbene has significant biological activities and great potential applications in pharmaceutical fields. The prepared nanoemulsion droplets are circular with smooth margin, and the mean size is 55.8±10.5 nm. The solubility, stability, and control release tests illustrated that the nanoemulsion delivery system dramatically improved the stability and solubility of pterostilbene, and *in vitro* release of pterostilbene was significantly improved in comparison to the pterostilbene suspension.

ACKNOWLEDGMENTS

We express our gratitude for the team fund of Hebei University of Science and Technology (XL201114, QD201211), Hebei Medical and Chemical Engineering Centre, and Pharmaceutical Molecular Chemistry Key Laboratory of Ministry Technology.

REFERENCES

1. Jeandet P, Breuil A, Adrian M, Weston L, Debord S, Meunier P, *et al.* HPLC analysis of grapevine phytoalexins coupling photodiode array detection and fluorometry. Anal Chem. 1997;69:5172–5.
2. Spath E, Schlager J. Constituents of red sandalwood. II. Constitution of pterostilbene. Berichte der Deutschen Chemischen Gesellschaft [Abteilung] B: Abhandlungen. 1940;73B:881–4
3. Seshadri TR. Polyphenols of Pterocarpus and Dalbergia woods. Phytochemistry. 1972;11:881–98.
4. Ghisalberti EL, Jefferies PR, Lanteri R, Matisons J. Constituents of propolis. Experientia. 1978;34:157–8.
5. Langcake P, Cornford C, Pryce R. Identification of pterostilbene as a phytoalexin from *Vitis vinifera* leaves. Phytochemistry. 1979;18:1025–7.
6. Mathew J, Rao A. Chemical examination of *Pterocarpus marsupium*. J Indian Chem Soc. 1984;61:728–9.
7. Rimando A, Cody R. Determination of stilbenes in blueberries. LCGC North America. 2005;23:1192, 1194, 1196, 1198, 1200.
8. Adrian M, Jeandet P, Douiller-Breuil A, Tesson L, Bessis R. Stilbene content of mature *Vitis vinifera* berries in response to UV-C elicitation. J Agric Food Chem. 2000;48:6103–5.
9. Wang X, Lu W, Chen J, Lu Y, Wu N, Kang W, *et al.* Studies on the chemical constituents of chloroform extract of *Dracaena cochinchinensis*. Yaoxue Xuebao. 1998;33(10):755–8.
10. King FE, King TJ, Manning LC. The Gibbs reaction and the constitution of jacareubin. J Chem Soc. 1957;51:563–6.
11. Paul B, Masih I, Deopujari J, Charpentier C. Occurrence of resveratrol and pterostilbene in age-old darakchasava, an Ayurvedic medicine from India. J Ethnopharmacol. 1999;68:71–6.
12. Perecko T, Drabikova K, Rackova L, Ciz M, Podborska M, Lojek A, *et al*. Molecular targets of the natural antioxidant pterostilbene: effect on protein kinase C, caspase-3 and apoptosis in human neutrophils in vitro. Neuroendocrinol Lett. 2010;31:84–90.
13. Chiou Y, Tsai M, Nagabhushanam K, Wang YJ, Wu CH, Ho CT, *et al*. Pterostilbene is more potent than resveratrol in preventing azoxymethane (AOM)-induced colon tumorigenesis via activation of the NF-E2-related factor 2 (Nrf2)-mediated antioxidant signaling pathway. J Agric Food Chem. 2011;59:2725–33.
14. Hougee S, Faber J, Sanders A, De J, Romy B, Wim B, *et al.* Selective COX-2 inhibition by a *Pterocarpus marsupium* extract characterized by pterostilbene, and its activity in healthy human volunteers. Planta Med. 2005;71:387–92.
15. Pan M, Chang Y, Badmaev V, Nagabhushanam K, Ho C. Pterostilbene induces apoptosis and cell cycle arrest in human gastric carcinomal cells. Food Chem. 2007;55:7777–83.
16. Ferrer P, Asensi M, Ramon S, Ortega A, Benlloch M, Obrador E, *et al*. Association between pterostilbene and quercetin inhibits metastatic activity of B16 melanoma. Neoplasia. 2005;7:37–47.
17. Tolomeo M, Grimaudo S, Cristina A, Roberti M, Pizzirani D, Meli M, *et al.* Pterostilbene and 3′-hydroxypterostilbene are effective apoptosis-inducing agents in MDR and BCR-ABL-expressing leukemia cells. Int J Biochem Cell Biol. 2005;37:1709–12.
18. Schneider J, Alosi J, McDonald D, McFadden D. Pterostilbene inhibits lung cancer through induction of apoptosis. J Surg Res. 2010;161:18–22.
19. Lee M, Pan M, Chiou Y, Cheng A, Huang H. Resveratrol modulates MED28 (magicin/EG1) expression and inhibits epidermal growth factor (EGF)-induced migration in MDA-MB-231. human breast cancer cells. J Agric Food Chem. 2011; Online Computer File.
20. Gutiérrez J, González C, Maestro A, Sole I, Pey C, Nolla J. Nanoemulsions: new applications and optimization of their preparation. Curr Opin Colloid Interface Sci. 2008;13:245–51.
21. Liu Y, Zhang D, Zou D, Wang Y, Duan C, Jia L, *et al.* Transmission of visible and ultraviolet light through charge-stabilized nanoemulsions. J Biomed Nanotechnol. 2011;7:621–31.
22. Szebeni J, Alving C, Savay S. Formation of complement-activating particles in aqueous solutions of Taxol: possible role in hypersensitivity reactions. Int J Immunopharmacol. 2001;1(4):721–35.
23. Gong Y, Wu Y, Zheng C, Fan L, Xiong F, Zhu J. An excellent delivery system for improving the oral bioavailability of natural vitamin E in rats. AAPS Pharm Sci Technol. 2012;13(3):961–6.
24. Chang L, Wu C, Liu C, Chuo W, Li P, Tsai T. Preparation, characterization and cytotoxicity evaluation of tanshinone IIA nanoemulsions. J Biomed Nanotechnol. 2011;7:558–67.
25. Desai NS, Nagarsenker MS. Design and evaluation of self-nanoemulsifying pellets of repaglinide. AAPS Pharm Sci Technol. 2013;14(3):994–1003.

26. Vandamme T, Anton N. Low-energy nanoemulsification to design veterinary controlled drug delivery devices. Int J Nanomedicine. 2010;5:867–73.
27. Wang L, Dong J, Chen J, Eastoe J, Li X. Design and optimization of a new self-nanoemulsifying drug delivery system. J Colloid Interface Sci. 2009;330:443–8.
28. Elnaggar Y, El-Massik M, Abdallah O. Sildenafil citrate nanoemulsion vs. self-nanoemulsifying delivery systems: rational development and transdermal permeation. Int J Nanotechnol. 2011;8(8/9):749–63.
29. Uso'n N, Garcia M, Solans C. Formation of water-in-oil (W/O) nano-emulsions in a water/mixed non-ionic surfactant/oil systems prepared by a low-energy emulsification method. Colloids Surf A Physicochem Eng Asp. 2004;250(1–3):415–21.
30. Porras M, Solans C, González C, Martinez A, Guinart A, Gutierrez J. Studies of formation of W/O nano-emulsions. Colloids Surf A Physicochem Eng Asp. 2004;249:115–8.
31. Wang L, Li X, Zhang G, Dong J, Eastoe J. Oil-in-water nanoemulsions for pesticide formulations. J Colloid Interface Sci. 2007;314:230–5.
32. Zhang Y, Zhao SC. Process for preparation of stilbene compounds by Kornblum oxidation, C.N.; 2010. Patent 101,838,173 Sep 22.
33. Bali V, Ali M, Ali J. Study of surfactant combinations and development of a novel nanoemulsion for minimizing variations in bioavailability of ezetimibe. Colloids Surf B: Biointerfaces. 2010;76:410–20.
34. Liu G, Zhang J, Wu P, Li J, Liu Y, Zhou X, *et al*. Preparation and evaluation of O/W pharmaceutical microemulsions. Zhongguo Nongye Kexue (Beijing, China). 2009;42(9):3328–33.
35. Chinese State Food and Drug Administration. Chinese Pharmacopoeia, 2010 ed. Appendix XIX c, Material medicine and pharmaceutical preparations stability experiment principle; Appendix V C, HPLC method; 2010.
36. Pan G, Jia X, Wei H. Comparison among several preparation methods for pseudo-ternary phase diagrams of pharmaceutical microemulsions. J Chin Pharm. 2006;17:21–3.
37. Sagitani H. Making homogeneous and fine droplet O/W emulsions using nonionic surfactants. J Am Oil Chem Soc. 1981;58:738–43.
38. Dai L, Li W, Hou X. Effect of the molecular structure of mixed nonionic surfactants on the temperature of miniemulsion formation. Colloids Surf A Physicochem Eng Asp. 1997;125:27–32.
39. Warisnoicharoen W, Lansley AB, Lawrence MJ. Nonionic oil-in-water microemulsions: the effect of oil type on phase behavior. Int J Pharm. 2000;198:7–27.
40. Lamaallam S, Bataller H, Dicharry C, Lachaise J. Formation and stability of miniemulsions produced by dispersion of water/oil/surfactants concentrates in a large amount of water. Colloids Surf A Physicochem Eng Asp. 2005;270–271:44–51.
41. Pons R, Carrera I, Caelles J, Rouch J, Panizza P. Formation and properties of miniemulsions formed by microemulsions dilution. Adv Colloid Interf Sci. 2003;106:129–46.